Institut de Physique Nucléaire de Lyon

Université Claude Bernard

IN2P3 - CNRS

LYCEN 2000/06
February 2000

Dynamical features in nucleus-nucleus collisions studied with INDRA

M-F. Rivet, et al., INDRA Coll.

International Symposium on Advances in Nuclear Physics
Bucarest (Roumanie) December 9-10, 1999
in Proceedings

43, Boulevard du 11 Novembre 1918 - 69622 VILLEURBANNE Cedex - France

DYNAMICAL FEATURES IN NUCLEUS-NUCLEUS COLLISIONS STUDIED WITH INDRA

M.F. RIVET[1], F. BOCAGE[2], B. BORDERIE[1], J. COLIN[2], P. LAUTESSE[3], J. LUKASIK[1]*, A.M. MASKAY[3], P. PAWŁOWSKI[1], E. PLAGNOL[1], G. AUGER[4], CH.O. BACRI[1], N. BELLAIZE[3], R. BOUGAULT[2], B. BOURIQUET[4], R. BROU[2], P. BUCHET[5], J.L. CHARVET[5], A. CHBIHI[4], D. CUSSOL[2], R. DAYRAS[5], N. DE CESARE[7], A. DEMEYER[3], D. DORÉ[5], D. DURAND[2], J.D. FRANKLAND[4], E. GALICHET[1,8], E. GENOUIN-DUHAMEL[2], E. GERLIC[3], S. HUDAN[4], D. GUINET[3], F. LAVAUD[1], J.L. LAVILLE[4], J.F. LECOLLEY[2], C. LEDUC[3], R. LEGRAIN[5], N. LE NEINDRE[2], O. LOPEZ[2], M. LOUVEL[2], L. NALPAS[5], J. NORMAND[2], M. PÂRLOG[6], J. PÉTER[2], E. ROSATO[7], F. SAINT-LAURENT[4]†, J.C. STECKMEYER[2], M. STERN[3], G. TĂBĂCARU[6], B. TAMAIN[2], L. TASSAN-GOT[1], O. TIREL[4], E. VIENT[2], M. VIGILANTE[7], C. VOLANT[5], J.P. WIELECZKO[4]
(INDRA COLLABORATION)

1 *Institut de Physique Nucléaire, IN2P3-CNRS, F-91406 Orsay Cedex, France.*
2 *LPC, IN2P3-CNRS, ISMRA et Université, F-14050 Caen Cedex, France.*
3 *Institut de Physique Nucléaire, IN2P3-CNRS et Université, F-69622 Villeurbanne Cedex, France.*
4 *GANIL, CEA et IN2P3-CNRS, B.P. 5027, F-14076 Caen Cedex, France.*
5 *DAPNIA/SPhN, CEA/Saclay, F-91191 Gif sur Yvette Cedex, France.*
6 *National Institute for Physics and Nuclear Engineering, RO-76900 Bucharest-Măgurele, Romania.*
7 *Dipartimento di Scienze Fisiche e Sezione INFN, Universiti Napoli 'Federico II", I-80126 Napoli, Italy.*
8 *Conservatoire National des Arts et Métiers, F-75141 Paris cedex 03.*

Dynamical emissions observed in heavy-ion collisions around the Fermi energy are reviewed. Their main interest lies in their connection with the in-medium nucleon-nucleon cross section (two-body nuclear viscosity, stopping of nuclear matter and transparency). Among non-equilibrium emissions, direct cluster production, and aligned fission are detailed. Fusion cross sections for a light system are reported.

1 Introduction

The ensemble of nuclear reactions occurring between two heavy ions colliding at energies between 20 and 100 MeV/u can be well studied thanks to

*permanent address: Institute of Nuclear Physics, ul. Radzikowskiego 152, 31-342 Kraków, Poland.
†present address: DRFC/STEP, CEA/Cadarache, F-13018 Saint-Paul-lez-Durance cedex, France.

4π arrays, among which INDRA [1] is one of the most powerful. In this energy domain, nucleon-nucleon collisions are less and less Pauli blocked and thus progressively overcome mean fields effects. Non-equilibrium (or dynamical) emissions become important, and their separation from emissions from thermalised objects should allow to extract fundamental information such as relaxation times, nuclear viscosity, in-medium σ_{nn} ...The classification as equilibrated or non-equilibrated emission is not obvious, as the intervening time scales are very similar: reaction times vary from 40 fm/c (peripheral collisions at 100 MeV/u) to 250 fm/c (central collisions at 30 MeV/u); the characteristic energy relaxation time is $\tau_{th} \sim$ 20-30 fm/c, independent of the incident masses and energy [2]; the life-time of a nucleus heated at T=5 MeV is around 50 fm/c [3]. Moreover the reaction times are long enough to allow the growth of fluctuations, leading to shape, volume, surface instabilities, either in the bulk of the system or in the overlap zone of the incident partners.

The dominant binary character of the collisions is now well established, most of them ending up with two hot (projectile-like PLF and target-like TLF) fragments in the exit channel [4]. In most of the reactions, one observes, besides particles which seems to originate from evaporation by these fragments, the emission of nucleons and light clusters with a parallel velocity intermediate between those of the two main fragments, and perpendicular velocities which can reach high values. Obviously these products are emitted in the early stages of the collisions, but many different processes can be invoked, such as direct emissions of nucleons or clusters, neck rupture, aligned fission ...Fusion processes vanish above 40-50 MeV/u. For light systems, phenomena similar to fusion-evaporation are still observed, while for heavy systems fusion-multifragmentation occurs. In this presentation, after some global quantitative estimates of the dynamical emissions we will focus on two well characterised processes among those giving rise to these products, namely direct emission of nucleons followed by coalescence, and aligned break-up of the projectile-like fragment. Then fusion cross sections for a light system will be discussed in the light of the stopping power of nuclear matter in dynamical simulations.

2 Global estimate and composition of dynamical emissions

If one defines dynamical emissions as all products but those coming from the isotropic evaporation of *PLF/TLF having reached thermodynamical and shape equilibrium*, then a global estimate of the mass lost in dynamical emissions can be tempted. Because of detection threshold effects one generally works on the PLF side only. Isotropic PLF evaporation is quantified and subtracted from

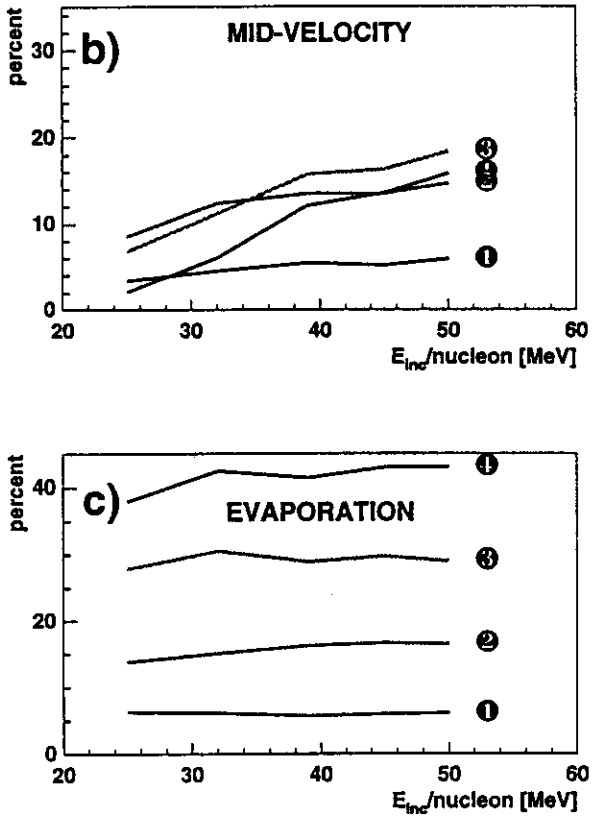

Figure 1. Xe+Sn system: Percentage of the forward detected charge emitted through dynamical (b) and evaporation (c) processes, as a function of incident energy. The numbers in black circles refer to an estimated (experimental) impact parameter, from peripheral (1) to mid-central (4). The heaviest (PLF) residue is not included, neither in b) nor in c). Extracted from [5].

the measured products, and the remaining part is attributed to dynamical emissions. The results, which strongly depend on the estimated PLF velocity (see refs [5,6] for more details) are shown in fig. 1 for the ^{129}Xe+^{nat}Sn system between 25 and 50 MeV/u. Dynamical emission becomes sizeable around 20 MeV/u, and significantly increases with energy, and with the centrality of the collision (curves labelled 1 to 4 correspond to average impact parameters from 9.2 to 4.7 fm); Conversely the evaporated charge increases with the centrality of the collisions, but appears to be independent of the energy *at a given impact parameter*: this could be interpreted as a saturation of the thermal excitation energy (*total, but not per nucleon*). For a lighter system, ^{36}Ar+^{58}Ni, the same evolution with centrality is observed, but there is no dependence on the energy between 52 and 95 MeV/u [6]. In this case the amount of charge attributed to dynamical emissions corresponds to the geometrical overlap of the incident

nuclei, at least for impact parameters larger than $b_{max}/2$.

Dynamical and statistical emissions so isolated strongly differ in their compositions. While protons and α particles dominate in evaporation, the other H, He isotopes and the light fragments mostly arise from other processes. Neutron rich fragments are more abundant in dynamical emissions [7], in a heavy system with a large neutron excess such as Xe+Sn, as well as in a light system with isospin close to 1, ^{36}Ar+^{58}Ni. It was suggested that this could result from the coalescence of small symmetric clusters, favored in the low density intermediate region, with the neutron rich gas simultaneously present [8,9]. A variant would be to view a stretched neck zone as a molecular cluster structure, such structures being stabilized by an excess of neutrons [10].

The equilibrium non-equilibrium separation so realised is very crude. Besides imposing drastic restrictions on what is qualified as evaporation (for instance deformed systems, density anisotropy of the semi-spaces backward and forward of the PLF due to the close proximity of the target, are not considered), it mixes in the "dynamical emissions" products whose origin and time of emission may be rather different. In the next two sections, we will focus on high energy particles, probably emitted very early, and on the aligned fission, which should be a process occurring later in the collision course.

3 High energy light charged particles: Coalescence of direct nucleons

The origins of high energy nucleons and light clusters in intermediate energy heavy ion collisions can be manyfold. It was proposed that they come from the fast ejection of nucleons or clusters preformed inside the nucleus [11], or from projectile break-up [12]. In the INDRA experiments, it was observed that protons and light clusters of high transverse energy are focused in the reaction plane [13]. This suggests angular momentum effects on nucleons ejected after a single collision; direct light clusters would then be formed through the coalescence of such nucleons. Coalescence naturally occurs in AMD simulations of heavy ion collisions, where it becomes more important than mean field effects for cluster formation when the incident energy increases [14]. Coalescence has been included in BUU calculations [15], leading to reasonable reproduction of some experimental light charged particles (lcp) spectra [16]. A revival of another approach was used in the INDRA collaboration. Direct nucleon densities in the momentum space given by an intranuclear cascade code (ISABEL [17], with $\sigma_{nn} = \sigma_{nn}^{free}$) were used as input of a coalescence model, instead of the measured nucleon spectra as previously done [18]. The calculation was intentionally limited to the cascade stage,without subsequent

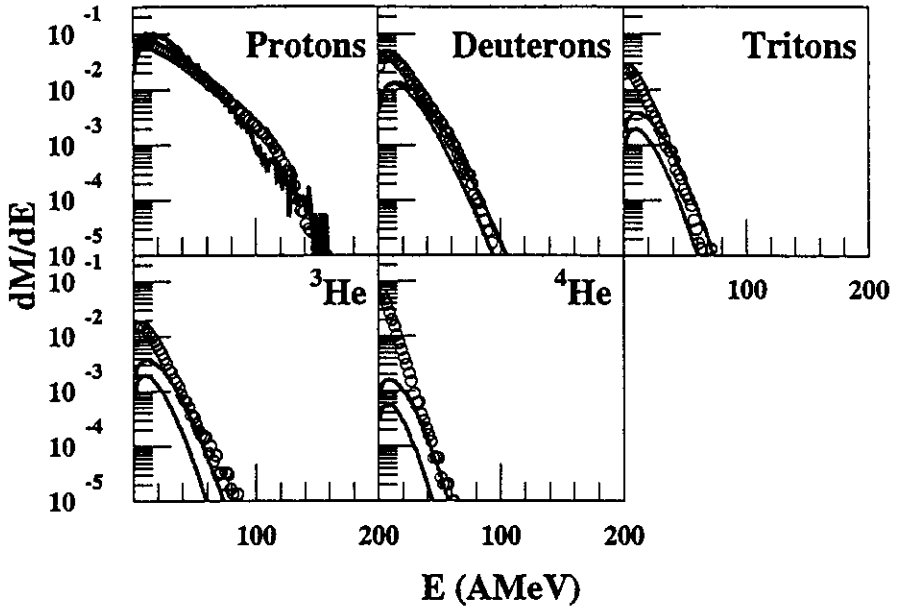

Figure 2. ^{36}Ar+^{58}Ni at 95 MeV/u: Comparison of the experimental (points) and calculated (lines) spectra of lcp emitted between 60 and 120°c.m. The double line for the calculation reflects uncertainties on the coalescence radius p_0. The impact parameter bin is 5-6 fm, and there is no normalisation factor. Extracted from [19].

evaporation. Comparison was done with the experimental spectra of lcp measured in the range 60-120°c.m. in the reaction ^{36}Ar+^{58}Ni at 95 MeV/u [19]; in this angular range, high energy particles appear more separated from the lcp evaporated by the PLF and TLF. Fig. 2 shows, for mid-peripheral collisions, that such a process quantitatively accounts for the higher energy part of the measured spectra (without any normalisation factor); the fraction of the lcp multiplicity which may arise from coalescence decreases when the particle mass increases (inherent to coalescence), and with decreasing centrality, due to smaller direct nucleon multiplicities.

4 Fission and aligned break-up of projectile-like fragments

For heavy projectiles ($Z_p > 40$) the binary break-up in two large fragments ("fission ") of the PLF, was studied in great details by the Nautilus and IN-

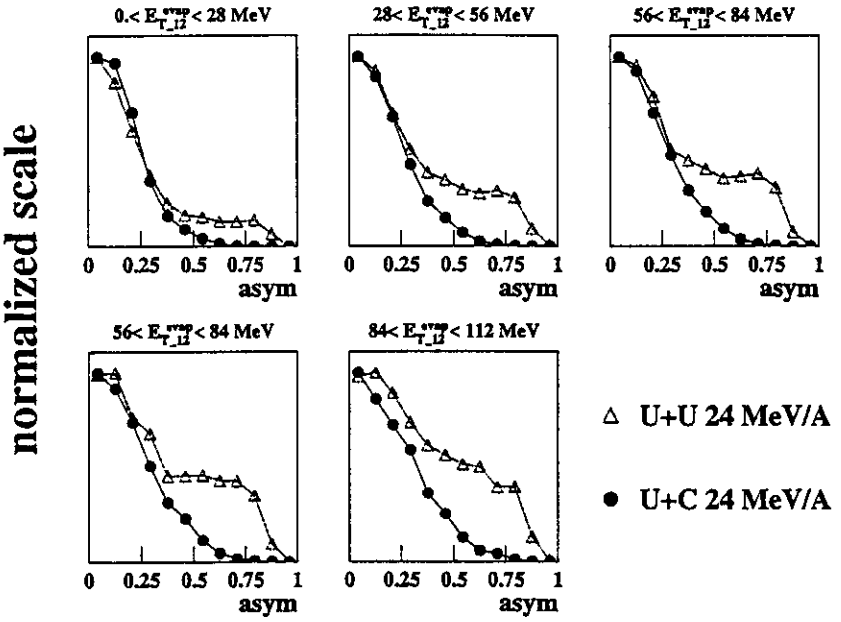

Figure 3. Fission fragment mass distributions (expressed vs asymmetry $\eta = (Z_1 - Z_2)/(Z_1 + Z_2)$ of a uranium projectile-like fragment after collisions with a U target (triangles) or a C target (points). The distributions are arbitrarily normalised at $\eta = 0$. Increasing $E^{evap}_{T_12}$ scale the impact parameter, from peripheral to mid-central collisions. Extracted from [20].

DRA collaborations [20], as it was in ref [21]. For a given projectile, "fission" mass distributions show striking differences depending on the bombarded target. Figure 3 illustrates this effect. A 24 MeV/u uranium colliding with a C target presents a "standard" fission distribution, where symmetric break-up dominates. When the target is a U nucleus, another component appears in addition to the previous one: it corresponds to an asymmetric break-up, and its relative importance increases with the centrality of the collision. The angular distributions of the two phenomena are also very different: while the scission axis is randomly oriented with respect to the recoil direction of the PLF, as expected, for standard fission, the asymmetric fission is strongly aligned on the PLF-TLF separation axis, and the smaller fragment is between the larger

partner and the TLF. The relative velocity of the fission fragments is much higher for aligned break-up. Aligned break-up was observed for different projectiles (Xe, Gd, Ta, Pb, U). Its relative weight in binary break-ups increases for decreasing fissility of the PLF, so as to become the dominant phenomenon for Xe-like PLF.

The privileged fission direction signs the memory of the dynamical part of the reaction, the PLF emerging from the nuclear reaction with a deformation already beyond the fission saddle point. Then an extra deformation velocity adds up to the "standard" (Coulomb + thermal) fission velocity. Such phenomena are important contributors to "dynamical" emissions. They are of primary interest in bringing information on the viscosity of nuclear matter in the intermediate energy domain.

5 Fusion cross sections

Incomplete fusion cross sections for light systems were found to vanish beyond 30-40 MeV/u [22,23]. Similar data have been obtained with INDRA for different systems, ^{36}Ar+KCl, ^{36}Ar+^{58}Ni, and ^{58}Ni+^{58}Ni, for which the fusion excitation function [24] is shown in fig. 4. At 32 MeV/u the fusion cross section has already dropped to 4-5% of the reaction cross section, and it represents less than 1% beyond 40 MeV/u. The occurrence of fusion is linked to the stopping power of nuclear matter, and thus depends on in-medium σ_{nn}. It is therefore a strong experimental constraint to test dynamical simulations. Recently Landau-Vlasov simulations were performed in order to determine the threshold energy E_{th} defined as the energy at which, for a given impact parameter, the system fuses below E_{th} and remains binary above [25]. The mean field was implemented through a Gogny force with K_∞=228 MeV, and the residual interaction was simulated with the free, energy and isospin dependent σ_{nn} arbitrarily scaled with a constant factor which was varied from 0. to 1.5. The Ni+Ni excitation function of fig. 4 puts, in a sharp cut-off picture, the threshold energy for b=2 fm at 37 MeV/u; from the simulations it would require a very high σ_{nn}, around 1.5 times σ_{nn}^{free}. Similar high σ_{nn} were required to reproduce the angular and velocity distributions of fragments produced in dissipative Ar+Ag collisions at 27 MeV/u *with the same simulation* [26]. The enhancement of σ_{nn} was suggested in calculations with the Brueckner G-matrix [27,28], and we feel that it is striking to need the same enhancement of σ_{nn} to reproduce data obtained on different exit channels with different experimental devices. For fusion data however, one should keep in mind that a sharp cut-off picture is unrealistic, and semi-classical simulations including fluctuations predict a non-negligible percentage of fusion events for

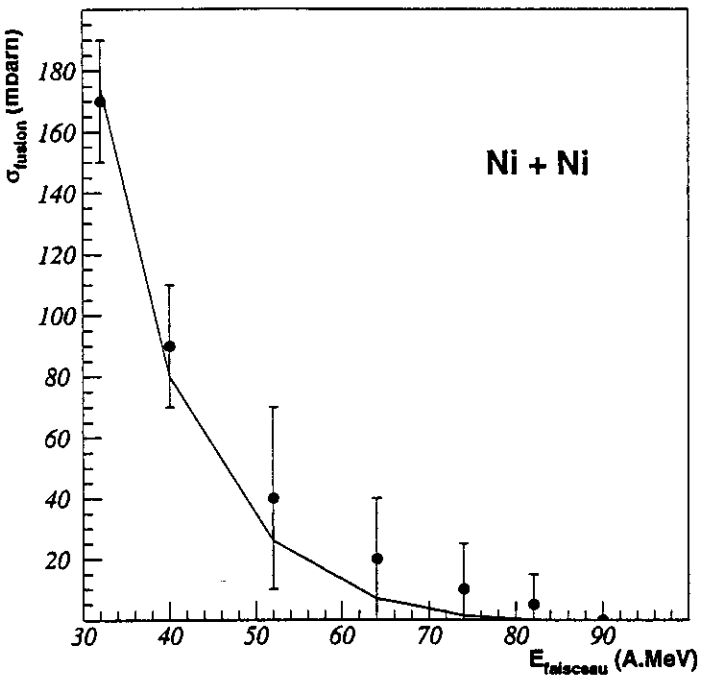

Figure 4. Fusion excitation function for the ^{58}Ni+^{58}Ni system. The points are experimental data and the line shows the prediction of the event generator SIMON. The abscissa axis is the lab. energy per nucleon. Extracted from [24].

rather large impact parameters [29].

6 Summary

In this paper we have touched on some dynamical features of heavy ion collisions which clearly stand out. Dynamical emissions may occur within different time scales, but can all be linked to the stopping (viscosity) of nuclear matter.The analyses presented here tempted to separate dynamical and statistical emissions. Such separations may be avoided if one only search to constrain the ingredients of transport models with experimental results, and approaches in this sense are underway [30].

References

1. J. Pouthas *et al.*, (INDRA coll.), *Nucl. Instrum. Methods* A **357**, 418 (1995).
2. B. Borderie *et al.*, *Z. Phys.* A **357**, 7 (1997).
3. B. Borderie, *Ann. Phys. Fr.* **17**, 349 (1992).
4. V. Métivier *et al.*, (INDRA coll.), *Nucl. Phys.* A , (in press).
5. E. Plagnol *et al.*, (INDRA coll.) *Phys. Rev.* C **61**, 014606 (1999)
6. T. Lefort *et al.*, (INDRA coll.), *Nucl. Phys.* A , (in press).
7. F.Dempsey *et al.*,PRC **54**, 1710 (1996).
8. L.G. Sobotka *et al.*,PRC **55**, 2109 (1997).
9. Ph. Chomaz and F. Gulminelli, PLB **447**, 221 (1999).
10. W. Von Oertzen, *Z. Phys.* A **357**, 355 (1997).
11. Chinmay Basu and Sudip Ghosg, *Phys. Rev.* C **56**, 3248 (1997).
12. H. Fuchs and K. Möhring, *Rep. Prog. Phys.* **57**, 231 (1994).
13. R. Dayras *et al.*, (INDRA coll.), unpublished data.
14. A. Ono, in *Proceedings of the 7th Conference on Clustering Aspects of Nuclear Structure and Dynamics* Rab, Croatia, 1999, (World Scientific).
15. P. Danielewicz *et al.*, *Nucl. Phys.* A **553**, 712 (1991) and *Phys. Rev.* C **46**, 2002 (1992).
16. D. Prindle *et al.*, *Phys. Rev.* C **57**, 1305 (1998).
17. Y. Yariv and Z. Fraenkel, *Phys. Rev.* C **20**, 2227 (1979) and *Phys. Rev.* C **24**, 488 (1981).
18. T.C. Awes *et al.*, *Phys. Rev.* C **24**, 89 (1981) and C **25**,2361 (1982).
19. P. Pawłowski *et al.*, (INDRA coll.), to be published.
20. F. Bocage *et al.*, (INDRA and Nautilus coll.), subm. to *Nucl. Phys.* A.
21. A. Stefanini *et al.*, *Z. Phys.* A **351**, 167 (1995).
22. A. Fahli *et al.*, *Phys. Rev.* C **34**, 161 (1986)
23. P. Box *et al.*, *Phys. Rev.* C **50**, 934 (1993)
24. A.M. Maskay, *thèse*, Université Lyon-1, LYCEN - T 9969.
25. Z. Basrak and P. Eudes in *Proceedings of the XXXVII International Winter Meeting on Nuclear Physics*, Bormio, 1999, edited by I. Iori (University of Milan Press, Milan, 1999).
26. F. Haddad *et al.*, *Z. Phys.* A **354**, 321 (1996)
27. A. Bohnet *et al.*, *Nucl. Phys.* A **494**, 349 (1989).
28. J. Cugnon *et al.*, *Phys. Rev.* C **35**, 861 (1987)
29. M.Colonna *et al.*, *Nucl. Phys.* A **642**, 449 (1998).
30. J.F. Lecolley *et al.*, (INDRA coll.), *Nucl. Instrum. Methods* A , (in press).